PHYSICAL REVIEW B VOLUME 22, NUMBER 4 15 AUGUST 1980

Decay kinetics of excitons and the electron-hole plasma in GaP:N

M. Sternheim* and E. Cohen*
Bell Laboratories, Murray Hill, New Jersey 07974
(Received 18 October 1979)

The lifetime of excitons bound to nitrogen, τ_e, and of the electron-hole plasma (EHP), τ_p, in GaP:N was studied as a function of the following parameters: temperature (2–100 K), excitation intensity, and nitrogen-doping level. The photoluminescence was excited both selectively and above the gap by using a pulsed, tunable dye laser with photon flux varying in the range of 10^{14}–10^{19} photons/cm^2 per pulse. The observed $\tau_e(T)$ for various excitation intensities was quantitatively fitted to a model which assumes the existence of saturable deep exciton and electron traps ("shunt paths"). An estimate of the concentration and capture cross section of these traps is obtained. In addition to the well-known exciton capture by the nitrogen, an additional free-electron–hole pair-capture process is observed. This occurs when the photoexcited electron-hole pair concentration is greater than that required for a Mott transition (so that no excitons are available). In crystals with nitrogen concentration greater than 10^{18} cm^{-3} and under intense photoexcitation (resonantly with the A line), the EHP is created and its lifetime is virtually temperature independent. In addition, $\tau_e \neq \tau_p$ for most of the temperature range studied. This indicates that particle exchange between EHP and exciton regions is small.

I. INTRODUCTION

The subject of decay kinetics of excitons bound to isoelectronic nitrogen impurities in GaP has been extensively studied.[1] There are two central problems which have not yet been fully resolved: (a) the determination of the relative probability of radiative recombination to nonradiative decay and the identification of decay channels; and (b) can a single nitrogen impurity bind an electron (thus becoming a Coulombic trap for the hole) or is an exciton the only entity to bind? The situation here is different from that of other isoelectronic centers in GaP, namely, Bi,[2,3] deep nitrogen pairs[4] ($NN_i, i=1,6$), and nearest-neighbor Zn-O pairs[5,6] where successive binding of electron and hole has been established.

Still another problem is that of exciton and electron-hole plasma (EHP) decay in GaP:N crystals which are excited by a strong light pulse (electron-hole densities exceeding 10^{18} cm^{-3}).[7,8] The main interest in this case is in the particle exchange between the plasma and the nitrogen impurities, and in whether a state of semiequilibrium is established between these subsystems.

In this paper we address ourselves to these problems. We report experimental results on the lifetime of excitons bound to nitrogen and of the EHP as a function of several controlled parameters: temperature, density of photoexcited particles, and nitrogen-doping level. The data are analyzed by solving the rate equations for all photoexcited particles and traps in the crystals. The results indicate that deep exciton and electron (or hole) traps, the so-called "shunt path", play an important role in the excitons' decay kinetics. The experimental method used here allows partial or full saturation of the shunt paths, thus providing an estimate of their concentration and capture cross section. It does not yield, however, any information on their energy levels, and in this aspect is different from the deep-level transient-spectroscopy (DLTS) method used by Henry and Lang.[9] The experimental results also show that nitrogen can bind free excitons as well as free-electron–hole pairs. In the latter case it is impossible to determine whether simultaneous or successive trapping occurs, but the process of free-carrier trapping is clearly identified. In the case of high excitation levels the decay kinetics of excitons bound to nitrogen and the EHP indicate that the two systems are not in a state of equilibrium.

Previous studies[10-12] of luminescence-decay kinetics of GaP:N involved mainly light-emitting diode (LED) materials and were performed at high temperatures. The emphasis there was on the influence of p or n doping on lifetime and radiative-recombination efficiency. In the present work we used crystals with low-background donor and acceptor concentrations and confined our studies to low temperatures ($2 \leq T \leq 100$ K) where the radiative recombination of excitons bound to nitrogen is efficient.

The paper is presented as follows. Section II describes the experimental technique and results. Section III describes the models used in data interpretation and discusses the parameters obtained by the analysis. Section IV summarizes the paper.

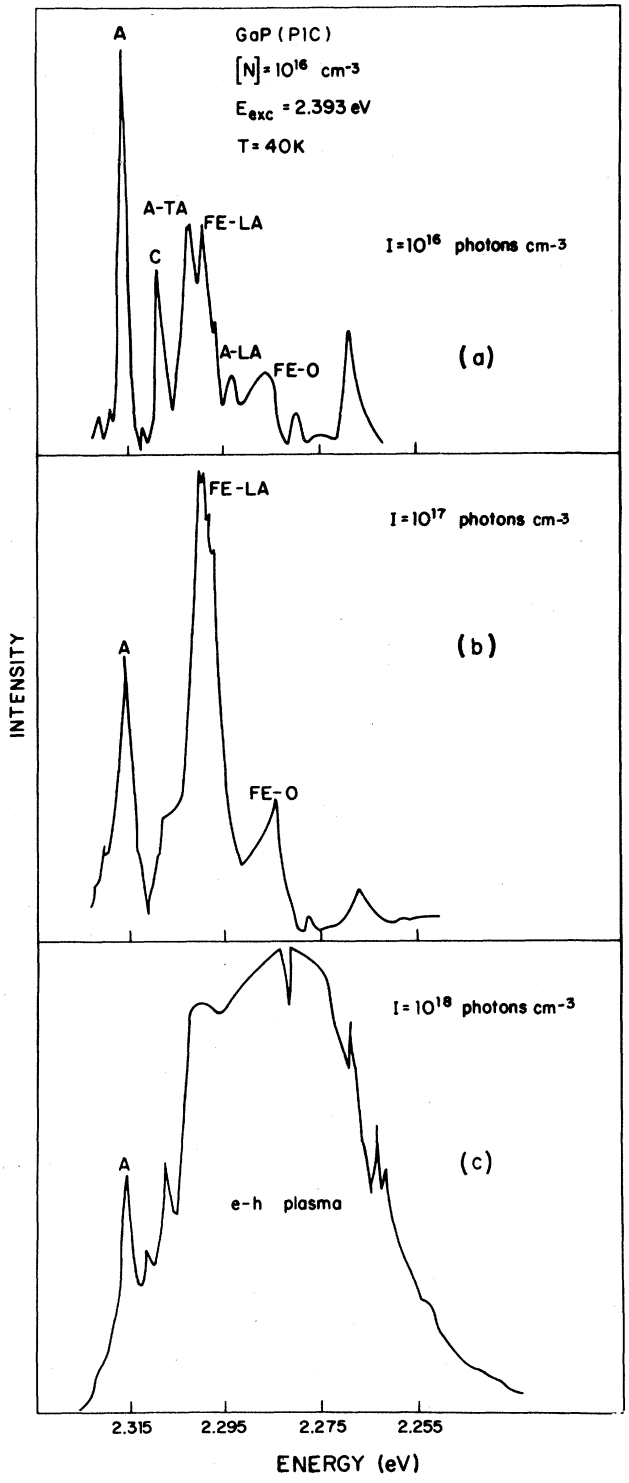

FIG. 1. Photoluminescence of a lightly doped GaP: N under various excitation intensities.

II. EXPERIMENTAL PROCEDURE AND RESULTS

The crystals used in this study were nitrogen doped in the bulk to the levels of $[N] = 10^{16} - 2 \times 10^{18}$ cm^{-3}. The background impurity level of unwanted donors or acceptors was less than 10^{16} cm^{-3}. The low-temperature photoluminescence of all crystals (excited with a low-level Ar^+ laser) did not show donor-acceptor pair spectra and only one showed a weak line due to excitons bound to neutral donors (C line).

The excitation source used for decay-kinetics studies was a tunable dye laser pumped with a N_2 laser. The pulse width varied from 2 nsec in the green to 4 nsec in the blue. The peak pulse power was 10 kW and the repetition rate used was 15 Hz. The laser linewidth was 0.2 meV. The crystals were mounted in a cryostat and cooled by a stream of cold He gas directed on them. The temperature was monitored with a thermocouple to an accuracy of 0.3 K. Temperature stabilization was ± 0.1 K. The crystals were front-surface excited, and their luminescence detected with a double monochromator equipped with a fast photomultiplier. The signals were processed with a boxcar averager with a gate of 1 nsec. The overall time resolution of the detection system was 6 nsec (limited by the photomultiplier response). The excitation density n_{exc} is taken as equal to the number of photons absorbed by the crystal per unit volume *per pulse*, I_0. It is estimated as follows. The number of photons per pulse is of the order of 10^{13}. The laser beam was focused down to a 10^{-3}-cm^2 spot or defocused up to a 0.5-cm^2 spot. The light-penetration depth is taken as the inverse absorption coefficient at the excitation wavelength.[13] The excitation density could be varied from $I_0 = 10^{14}$–10^{19} photons/cm^3 per pulse by changing the laser wavelength and the spot size, and by attenuation.

The experimental results can be divided into two main categories:

(a) For crystals with $[N] \lesssim 10^{17}$ cm^{-3} and excitation densities $n_{exc} \lesssim 10^{17}$ cm^{-3} the photoluminescence spectra are due to the radiative recombination of excitons bound to N and are similar to those obtained with low-level cw-laser excitation [Fig. 1(a)]. For $[N] \lesssim 10^{16}$ cm^{-3} and $n_{exc} \sim 10^{17}$ cm^{-3} the phonon-assisted recombination of free excitons can also be observed for $T \gtrsim 40$ K [Fig. 1(b)]. (b) for $[N] > 10^{17}$ cm^{-3} and $n_{exc} > 10^{17}$ cm^{-3} the spectra show the optical phonon-assisted recombination of excitons bound to N (A-O line) and a broad band due to the EHP [Figs. 1(c) and 2(b)]. The low-excitation-density spectrum of crystals with $[N] > 10^{18}$ cm^{-3} shows the NN_i lines in addition to the A-O line [Fig. 2(a)].

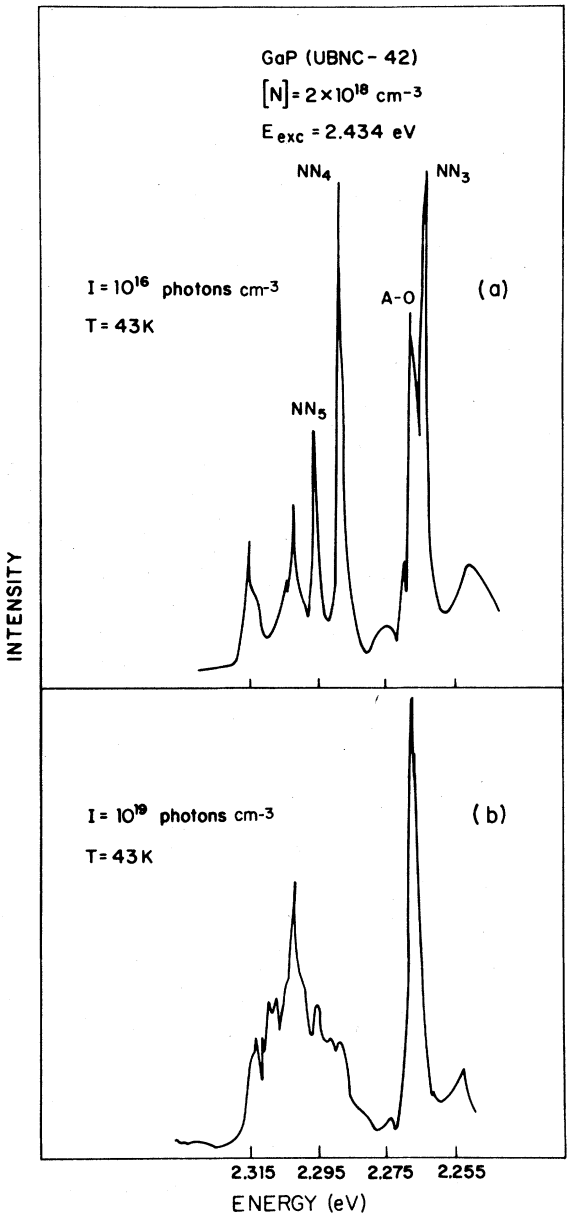

FIG. 2. Photoluminescence of a heavily doped GaP: N under low (a) and high (b) excitation intensities. The broad band ranging from 2.29–2.32 eV in b is the EHP radiative recombination.

The spectra change markedly at the doping level of $\sim 10^{17}$ cm^{-3}. Figure 3 compares the spectra of two crystals both having very similar nitrogen doping and excited at exactly the same conditions. The lighter-doped crystal shows mainly the spectrum of excitons bound to N (and some weak NN_i lines), while the more heavily doped crystals shows the broad band due to EHP in addition to the A-O line.

The lifetimes of all the observed spectral components (free excitons, excitons bound to N, and EHP) were measured as a function of n_{exc} and T. The results are shown in Figs. 4–6 for three different doping levels. All crystals show a similar behavior for $T \lesssim 20$ K and $n_{exc} \lesssim 10^{15}$ cm^{-3}. For $T < 10$ K the $\tau(T)$ curve is essentially the bound-exciton radiative-recombination lifetime.[14] For $10 < T < 20$ K the $\tau(T)$ curves follow an exponential dependence: $\tau(T) = \tau_0 \exp(-\Delta E/kT)$, with $\Delta E = 10 \pm 1$ meV. This exponential drop can be eliminated and $\tau(T)$ then reverts to a value close to the radiative lifetime by increasing the excitation density. For $10 < T < 40$ K the exponential drop of $\tau(T)$ can again be observed. The temperature at which the drop commences depends on [N] and on n_{exc}. The crystal doped with $[N] = 10^{17}$ cm^{-3} shows an exponential dependence with $\Delta E = 25 \pm 5$ meV in addition to the 10 ± 1 meV observed at lower T. The observed activation energies for all the spectral components and for different temperatures are summarized in Table I.

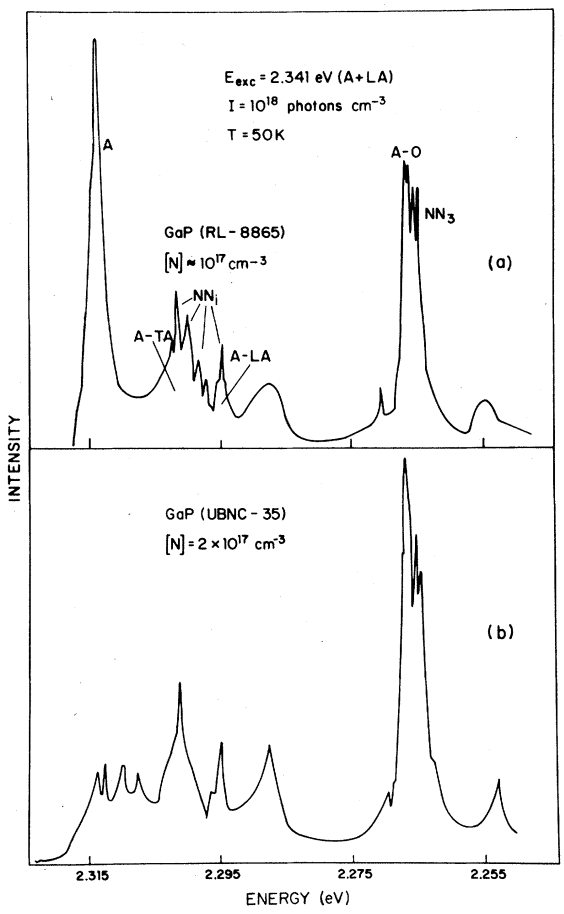

FIG. 3. Photoluminescence of two GaP: N crystals with intermediate doping levels taken under identical conditions. The absence of the A line in b is due to self-absorption.

TABLE I. Activation energies for the photoluminescence decay of the various spectral components.

[N] Transition	10^{16} cm^{-3}	10^{17} cm^{-3}	$>10^{17}$ cm^{-3}
A line	10 meV $10<T<40$ K	10 meV $10<T<20$ K 25 ± 5 meV $25<T<100$ K	10 meV $10<T<100$ K
Free exciton (FE)	10 meV $10<T<85$ K	Not observed	Not observed
EHP	15 meV $85<T<170$ K	Not observed	~2 meV $2<T<60$ K

III. ANALYSIS

A. Low excitation intensities

In this subsection we deal with analysis of $\tau(n_{exc}, T)$ in the case of $n_{exc} \lesssim 10^{16}$ cm^{-3} per pulse. Two general conclusions can be drawn from the experimental results. First, under low-level pulse excitations and for crystals with [N] $\lesssim 10^{17}$ cm^{-3}, the dominant radiative recombination is that of excitons bound to single nitrogen impurities. For [N] $> 10^{17}$ cm^{-3}, both isolated N and NN_i lines are observed. Second, the sets of $\tau(n_{exc}, T)$ curves demonstrate the existence of saturable deep traps (shunt paths) which act as nonradiative decay centers and drain part of the photoexcited particles. By analyzing these curves we shall arrive at a set of parameters which describe the system of excitons, electrons, holes, and their capture by both nitrogen centers and the deep traps.

The models used for the analysis are shown schematically in Fig. 7 and rest primarily on the following assumptions:

(a) At all times after the excitation pulse a state of quasiequilibrium exists between all photoexcited particles.[15] The shunt paths, whether exciton- or electron (hole)-trapping centers, are assumed to be much deeper than kT and thus do not thermalize with the free-particle bands.

(b) The nitrogen isoelectronic center acts mainly as an exciton trap (as shown in Fig. 7). However, as will be discussed below, it can also capture an electron-hole pair out of the free-particle bands (when the temperature is high so that the concentration of free excitons is small.)

(c) Two types of shunt paths have to be invoked: an exciton shunt shown schematically in Fig. 7 (a) and an electron (hole) shunt shown in Fig. 7(b). The exact order of trapping in the latter is unknown and the assumption made here of an electron captured first is arbitrary. It is clear that using just two types of deep centers (shunts) is

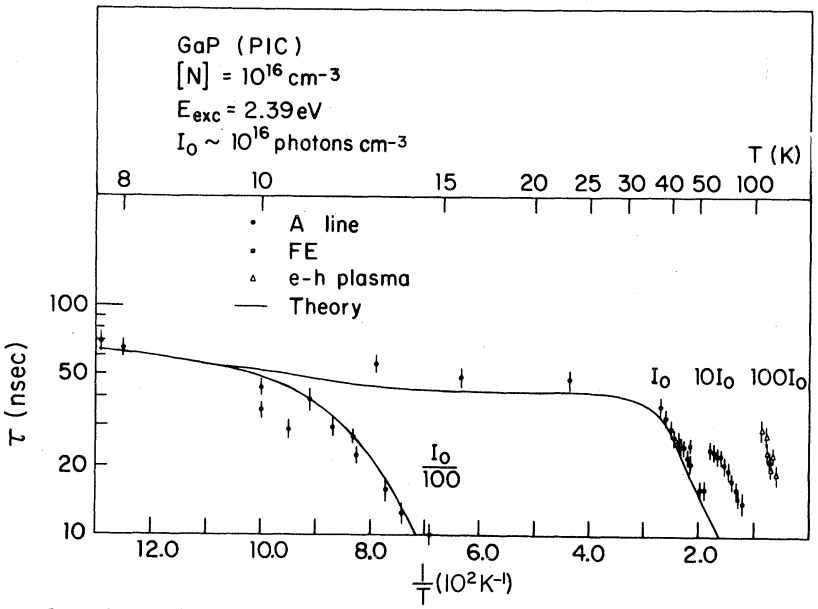

FIG. 4. Temperature dependence of the lifetime of the N-bound exciton, free exciton, and EHP under various excitation intensities for a lightly doped GaP:N.

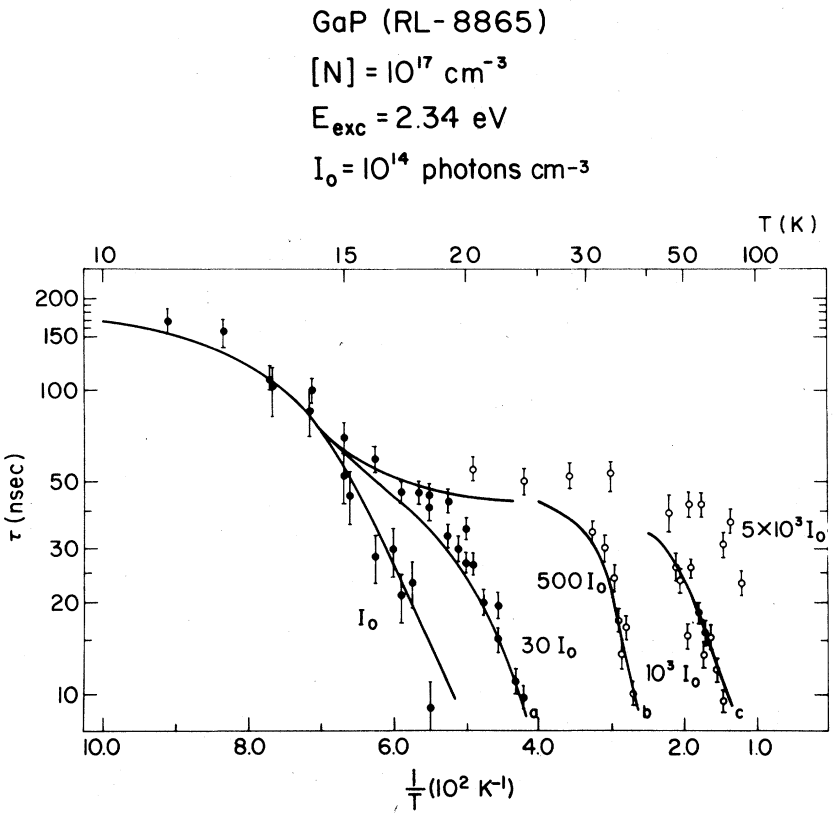

FIG. 5. Temperature dependence of the N-bound-exciton lifetime under various excitation intensities for an intermediately doped GaP: N.

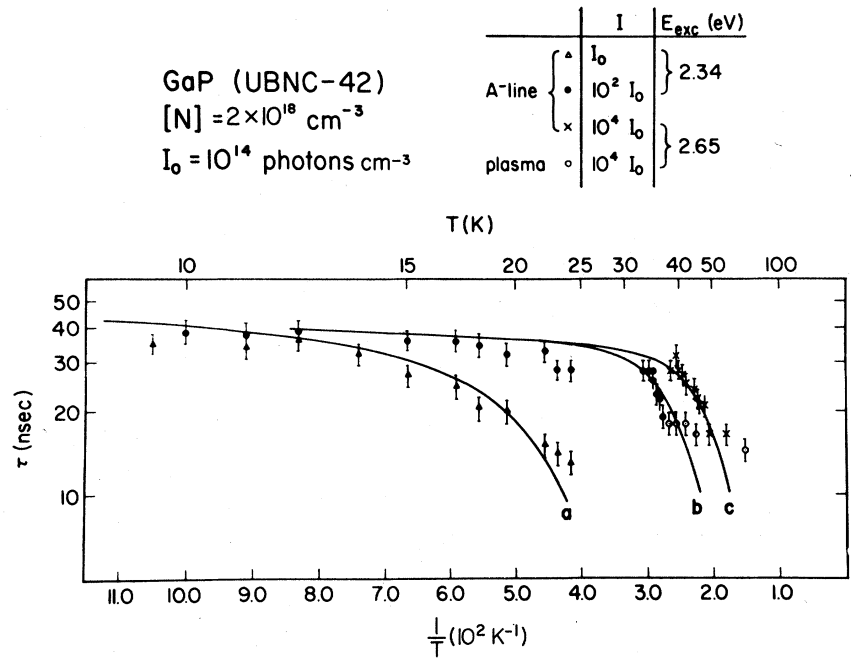

FIG. 6. Temperature dependence of the lifetime of the N-bound exciton and EHP under various excitation intensities for a heavily doped GaP: N.

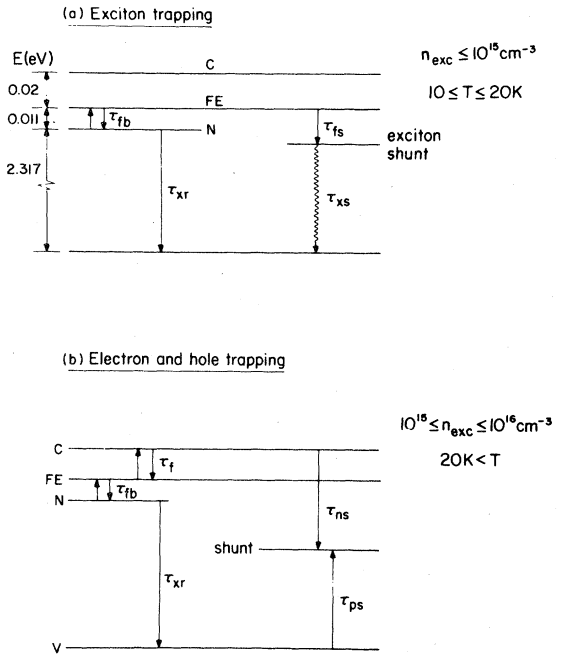

FIG. 7. Schematic description of the trapping processes of excitons on nitrogen and of excitons (a) and electron-hole pairs (b) on deep traps (shunts). The indicated temperature ranges apply only to crystals with $[N] \lesssim 10^{17}$ cm^{-3}.

an oversimplification of the actual case. However, it is found to provide a simple and clear description of exciton dynamics in the limit of low excitation levels.

Consider now the temperature range of $T \lesssim 20$ K. Cuthbert and Thomas[14] have shown that the radiative lifetime of excitons bound to N can be described by a thermal equilibrium between the B ($J=2$) and A ($J=1$) levels:

$$\tau_{xr} = \frac{\tau_B[1+\frac{3}{5}\exp(-\Delta E/kT)]}{1+\frac{3}{5}(\tau_B/\tau_A)\exp(-\Delta E/kT)} . \quad (1)$$

Here $\Delta E = 0.8$ meV and $\tau_B/\tau_A = 105$. τ_B was measured to be 4 μsec. However, internal strain admixes the two levels, thereby shortening τ_B. In this work we have determined τ_B for each crystal by measuring the radiative-recombination lifetime for $T < 10$ K and fitting it to Eq. (1).

Since the binding energy of free excitons is $E_f = 22 \pm 2$ meV (Ref. 16) and the additional binding energy of excitons to N is $E_b = 11$ meV, in the range of $10 < T \lesssim 20$ K the photoexcited crystal contains mainly free and bound excitons, with concentrations x_f and x_b per unit volume, respectively. Then, the exciton kinetics is affected solely by the presence of exciton shunts. If the excitation level is low ($n_{exc} \sim 10^{14}$ cm^{-3}) the shunts are empty and, upon increasing T, excitons escape from N and are captured by the shunts. This causes the quenching of photoluminescence as T increases and shortens τ. We denote by N the concentration of nitrogens and by K_x that of exciton shunts (K_x^0 of which are empty). The characteristic exciton-trapping times are denoted by τ_{fb} for N traps and τ_{fs} for the shunts, and the time the exciton resides on the shunt before recombining is denoted τ_{xs}. Then the model described by Fig. 7(a) can be formulated as follows[5]:

$$\begin{aligned}
\dot{x}_b &= -\frac{1}{\tau_{xr}} x_b + \frac{1}{\tau_{fb}} x_f\left(1-\frac{x_b}{N}\right) \\
&\quad - \frac{1}{\tau_{fb}} x_b \frac{N_x}{N g_b} \exp\left(-\frac{E_b}{kT}\right), \\
\dot{x}_f &= -\frac{1}{\tau_{fb}} x_f\left(1-\frac{x_b}{N}\right) + \frac{1}{\tau_{fb}} x_b \frac{N_x}{N g_b} \exp\left(-\frac{E_b}{kT}\right) \\
&\quad - \frac{1}{\tau_{fs}} x_f \frac{K_x^0}{K_x}, \\
\dot{K}_x^0 &= \frac{1}{\tau_{xs}}(K_x - K_x^0) - \frac{1}{\tau_{fs}} x_f \frac{K_x^0}{K_x} .
\end{aligned} \quad (2)$$

Here $g_b = 8$ is the bound-exciton degeneracy and $N_x = 4(2\pi m_x kT/h^2)^{3/2}$ is the free-exciton density of states. In the above rate equations we have neglected the very weak radiative recombination of free excitons and the nonradiative (i.e., multiphonon or escape by tunneling) of bound excitons. Capture cross sections σ are related to the trapping times by

$$\sigma = 1/v\tau K , \quad (3)$$

where K (or N) is the concentration of the trapping center and v is the thermal velocity of particles.

The set of equations (2) are integrated numerically for each value of n_{exc} and T. For the lowest excitation density, $n_{exc} = I_0 = 10^{14}$ cm^{-3}, the calculated $\tau(T)$ is shown in Figs. 4–6. We assume that the exciton-capture cross section on the nitrogen, σ_N, to be of the order of 10^{-10} cm^2.[17] Since for low excitation levels most of the exciton shunts are empty ($K_x^0/K_x \sim 1$) the only parameters left to be fit are τ_{fs} and τ_{xs}. The values obtained by the fit are given in Table II for the three nitrogen-doping levels. The concentration of exciton shunts K_x can be estimated by observing the lowest excitation density which suffices to saturate the shunts. This value turns out to be between 10^{15} and 10^{16} cm^{-3}. All the parameters of the exciton-trapping model are summarized in Table II.

Consider now the case of $[N] = 10^{17}$ cm^{-3} and excitation density $I_0 = 3 \times 10^{15}$ cm^{-3} shown in Fig. 5. At this excitation-density level the exciton shunts are saturated, yet a drop in $\tau(T)$ is clearly observed between 15–25 K. A calculation of $\tau(T)$

TABLE II. Parameters describing decay kinetics.

Temp. range	Type of trap	Symbol	Units	*P1C* [a]	*RL*8865 [a]	*UBNC*-42 [a]
	Nitrogen	[N]	cm^{-3}	10^{16}	10^{17}	10^{18}
0 K< T	trap	τ_B	sec	1.1×10^{-6}	3.35×10^{-6}	0.85×10^{-6}
		τ_{fb}	sec	3×10^{-13}	3×10^{-14}	2×10^{-15}
		σ_N	cm^2	10^{-10}	10^{-10}	10^{-10}
	Exciton	τ_{fs}	sec	8×10^{-11}	1.4×10^{-10}	6×10^{-11}
	shunt	K_x	cm^{-3}	3×10^{15}	10^{15}	5×10^{15}
10< T<25 K		σ_x	cm^2	3.5×10^{-12}	6×10^{-12}	2.8×10^{-12}
		τ_{xs}	sec	2×10^{-7}	4.8×10^{-8}	
	Electron	τ_{ns}	sec		3×10^{-12}	
	shunt	K_e	cm^{-3}		3×10^{15}	
		σ_e	cm^2		2.2×10^{-11}	
		τ_{ps}	sec		10^{-8}	
	Electron	τ_{ns}	sec	3.5×10^{-9}		5×10^{-10}
25 K< T	shunt	K_e	cm^{-3}	3×10^{15}		10^{16}
		σ_e	cm^2	2.3×10^{-14}		5×10^{-14}
		τ_{ps}	sec	3.5×10^{-9}		1.1×10^{-9}

[a] These are the names of the crystals used which were grown at Bell Labs.

for $I_0=3\times10^{15}$ cm^{-3} using exciton shunts only yields the curve which shows saturation at about 20 K (Fig. 5). Now at the temperature range of 15–25 K the concentration of free electrons and holes is sufficiently high ($\sim10^{10}$ cm^{-3}) that their capture at deep centers becomes the dominant quenching mechanism. The model describing this case is shown schematically in Fig. 7(b). We assume that the nitrogen centers capture free excitons only, and that these have a dissociation probability of $1/\tau_f$ per unit time. We assume (somewhat arbitrarily) that the shunts capture an electron first and then a hole. The concentration of shunts is K_e and they can exist in either one of two states, empty (concentration K_e^0) and electron occupied. This means that the electron-occupied trap is a recombination center for holes. The probabilities per unit time for an electron to be captured by an empty shunt is $1/\tau_{ns}$ while that of a hole (at an electron-occupied shunt) is $1/\tau_{ps}$. The rate equations appropriate for this model are

$$\begin{aligned}
\dot{x}_b &= -\frac{1}{\tau_{xr}}x_b+\frac{1}{\tau_{fb}}x_f\left(1-\frac{x_b}{N}\right)\\
&\quad-\frac{x_b}{\tau_{fb}}\frac{N_x}{Ng_b}\exp\left(-\frac{E_b}{kT}\right),\\
\dot{x}_f &= -\frac{1}{\tau_{fb}}x_f\left(1-\frac{x_b}{N}\right)+\frac{1}{\tau_{fb}}x_b\frac{N_x}{Ng_b}\exp\left(-\frac{E_b}{kT}\right)\\
&\quad-\frac{1}{\tau_f}x_f+\frac{np}{c\tau_f},\\
\dot{n} &= \frac{1}{\tau_f}x_f-\frac{np}{c\tau_f}-\frac{1}{\tau_{ns}}n\frac{K_e^0}{K_e},\\
\dot{p} &= \frac{1}{\tau_f}x_f-\frac{np}{c\tau_f}-\frac{1}{\tau_{ps}}\left(1-\frac{K_e^0}{K_e}\right).
\end{aligned}\tag{4}$$

The electrical neutrality condition is

$$K_e^0=K_e-(p-n)\,,\tag{5}$$

and c is the equilibrium rate constant[18] for the systems of free excitons and free electrons and holes:

$$c=\left(\frac{2\pi m_e m_h}{h^2 m_x}kT\right)^{3/2}\exp\left(-\frac{E_f}{kT}\right).\tag{6}$$

It is clear that for temperatures above 15 K both exciton and electron shunts will be effective and therefore a combination of the two sets of equations, (2) and (4), must be simultaneously solved. We do this for the crystal having $[N]=10^{17}$ cm^{-3} and the results are shown in Fig. 5 (the curve corresponding to 30 I_0). The two parameters which are fit by this curve are τ_{ns} and τ_{ps}. The concentration of shunts K_e is estimated from the excitation density required to obtain saturation.

It should be noted that the hole-capture time τ_{ps}, is not a sensitive fitting parameter. Under the excitation conditions used here, most of the shunts are empty. Then it is the primary particle (electron) capture which dominates the exciton kinetics. The parameters obtained by this procedure are given in Table II. It should be noted that in the case of high nitrogen doping (Fig. 6), saturation of either type of shunts occurs for an excitation density of 10^{16} cm^{-3}. For $T>30$ K, a drop in $\tau(T)$ is observed but its behavior is affected by the formation of an EHP, and will be discussed below.

Finally we turn to an interesting observation shown in Fig. 5 for $[N]=10^{17}$ cm^{-3} and $T\gtrsim30$ K (curves b and c). For excitation densities $n_{exc}>5\times10^{16}$ cm^{-3}, the emission is still dominated

TABLE III. Parameters used to fit the electron-hole capture process.

N parameters:		
[N]		10^{17} cm^{-3}
Electron-binding energy		2 meV
Hole-binding energy		27 meV
Electron-trapping time		10^{-10} sec
Hole-capture cross section		$2\times10^{-11}/T$ cm^2
Shunt parameters:		
Temperature range	35–45 K	45–60 K
τ_{ns}	2×10^{-12}	2×10^{-10} sec
K_e	10^{16}	10^{15} cm^{-3}
σ_e	10^{-11}	10^{-12} cm^2
τ_{ps}	10^{-8}	10^{-8} sec

by excitons bound to single nitrogen impurities, but the activation energy of its lifetime is $\Delta E = 25 \pm 5$ meV. This large energy is close to the binding energy of an electron-hole pair to the nitrogen ($E = E_f + E_b = 32$ meV). n_{exc} for which this phenomenon occurs is $n_c = kT/(16\pi E_f a_0^3) = 4\times10^{16}$ cm^{-3}, the critical density at which a Mott transition takes place (at 30 K).[19] This means that the nitrogen impurities trap electron-hole pairs *directly* from the free-particle bands. Electron-hole pairs can also be trapped by deep nonradiative traps. The fact that their saturation depends on excitation densities and on temperature indicates that there are several such traps. In order to analyze this phenomenon, one has to assume a mechanism for trapping electron-hole pairs by the nitrogen directly from the plasma. The two simplest models are (i) the consecutive-binding model (the electron is trapped by the bare nitrogen impurity and the hole binds by the Coulomb interaction), and (ii) the simultaneous-binding model (which requires the electron and hole to be simultaneously present in the nitrogen vicinity). We have tried fitting curves b and c of Fig. 5 using both models and found that the consecutive-binding one yielded a better agreement with experiment. The equations describing this model have been presented in a previous calculation[20] and the parameters obtained by fitting the present data are given in Table III. Two sets of traps are assumed, each with a different electron-capture cross section. Although the consecutive-binding model yielded a better fit to the lifetime data, the small electron binding energy (2 meV) is actually an indication that the electron cannot bind alone ($kT \sim 5$ meV in the temperature range for which curves b and c were observed). It seems that the hole presence near the nitrogen is required for binding an electron-hole pair. In spite of the satisfactory fit to the data, this model is an over simplification of a complex situation near n_c. We must conclude that the small electron binding energy is an indication that the electron cannot bind separately, in accordance with the spectroscopic observation.[4]

B. High excitation densities

In this subsection we analyze the decay kinetics of excitons bound to nitrogen in the presence of the EHP. Our aim is to determine to what degree there is particle exchange between these systems. For this it is best to study the data of the sample with $[N] = 2\times10^{18}$ cm^{-3}. As reported in Ref. 7, in this case the EHP can be created by resonantly pumping into the A line (2.34 eV), and it shows a strong no-phonon radiative-recombination band. (The crystals with $[N] \sim 10^{17}$ cm^{-3} do not show a plasma band, while that with $[N] = 10^{16}$ cm^{-3} shows only a very weak A line when the plasma is present and its lifetime is hard to measure). Figure 6 shows the A-line lifetimes in the presence of the EHP (that is, for $n_{exc} > 10^{18}$ cm^{-3}). The plasma lifetime is essentially temperature independent, $\tau_p \sim 18$ nsec for $T > 30$ K, and is slightly dependent on n_{exc}, as it is determined by the Auger effect.[7] The temperature dependence of the bound-exciton lifetime is similar to that observed for low [N] crystals, showing an activation energy of 10 meV. The spectroscopic data (Fig. 3), the large disparity between the exciton and EHP lifetimes, and their distinct dependence on temperature indicate that the particle exchange between the two systems is very small.

This observation can be tested quantitatively by solving the rate equations for the excitons and EHP. We first solved them for excitons bound to nitrogen assuming no particle exchange with the EHP. The appropriate set of equations are Eqs.

(2) and these were solved for curves b and c of Fig. 6. The parameters used for fitting the data are given in Table II. For both cases we assume that the exciton phase is in a state of quasi-equilibrium with initial exciton concentrations of 10^{16} and 10^{17} cm^{-3} for curves b and c, respectively. The calculated $\tau(T)$ fit well the observed data points.

We also tried to fit curves b and c by assuming a free exchange of particles between the EHP and bound-exciton phases. The mechanism of exchange is via the free excitons which evaporate from the plasma region.[21] Solving the coupled sets of rate equations requires a density of bound excitons in the range of 10^{18} cm^{-3} and the $\tau(T)$ curves could not be reproduced.

IV. SUMMARY

In this work we have studied the luminescence-decay kinetics of excitons bound to nitrogen and the electron-hole plasma in GaP:N. Since excitons bound to nitrogen do not decay by the Auger process (as do excitons bound to neutral donors and acceptors) they are particularly useful to probe nonradiative decay channels. We find that the data can be satisfactorily analyzed by assuming the existence of deep-exciton and free-particle traps (shunt paths) in the crystal. These traps can be saturated by applying a sufficiently intense light pulse, thus creating a large number of electron-hole pairs. The data enabled us to estimate the concentration and capture cross sections of these traps: exciton and electron-shunt concentration varies between 10^{15} and 10^{16} cm^{-3}. The exciton-capture cross section is very large, $\sim 10^{-12}$ cm^2. This should be compared with exciton capture on the nitrogen, $\sigma_N \sim 10^{-10}$ cm^2. We could assume that the exciton shunts are actually nitrogen pairs, but this would hold only for the high [N] samples. The electron-capture cross section varies between 10^{-14} and 10^{-11} cm^2 for the samples studied. The experimental method employed here does not yield any information on the energy-level structure of these deep traps.

The nitrogen impurities are found to capture both excitons and electron-hole pairs. The latter process occurs when there are no excitons available and only free particles can be captured. This appears to be the case when the density of photoexcited excitons is greater than that required for a Mott transition. The mechanism of capture by nitrogen is not clear, although the luminescence-decay data could be better fit assuming consecutive electron and hole binding (rather than simultaneous binding). Finally, it is found that the lifetimes of the EHP and of the excitons bound to nitrogen are disparate for any temperature below ~100 K. The two subsystems decay without a significant particle exchange between them. This may indicate that the EHP is confined in space to pockets which do not exchange particles with the surrounding exciton-filled space. In GaP:N this happens even when the plasma is created by condensation of excitons bound to nitrogen (i.e., by selective excitation into the A line). The reason for the lack of thermalization between the bound excitons and the EHP may be due to the short plasma lifetime. This problem could be better tackled by the use of short-pulse techniques (< 1 nsec).

ACKNOWLEDGMENT

The technical assistance of H. Katz is greatly appreciated.

---

*Permanent address: Department of Physics and Solid State Institute, Technion, Haifa, Israel.

[1] A. A. Bergh and P. J. Dean, *Light-emitting Diodes* (Clarendon, Oxford, 1976).
[2] J. J. Hopfield, D. G. Thomas, and R. T. Lynch, Phys. Rev. Lett. 17, 312 (1966).
[3] P. J. Dean, J. D. Cuthbert, and R. T. Lynch, Phys. Rev. 179, 754 (1969).
[4] E. Cohen and M. D. Sturge, Phys. Rev. B 15, 1099 (1977).
[5] J. M. Dishman and M. DiDomenico, Jr., Phys. Rev. B 1, 3381 (1970).
[6] C. H. Henry, P. J. Dean, and J. D. Cuthbert, Phys. Rev. 166, 754 (1968).
[7] J. E. Kardontchik and E. Cohen, Phys. Rev. B 19, 3181 (1979).
[8] R. Schwabe, F. Thuselt, H. Weinert, and R. Bindemann, J. Lumin. 18/19, 537 (1979).
[9] C. H. Henry and D. V. Lang, Phys. Rev. B 15, 989 (1977).
[10] R. Z. Bachrach and O. G. Lorimor, J. Appl. Phys. 43, 500 (1972).
[11] P. D. Dapkus, W. H. Hackett, Jr., D. G. Lorimor, G. W. Kammlot, and S. E. Haszko, Appl. Phys. Lett. 22, 227 (1973).
[12] P. D. Dapkus, W. H. Hackett, Jr., D. G. Lorimor, and R. L. Bachrach, J. Appl. Phys. 45, 4920 (1974).
[13] J. J. Hopfield, P. J. Dean, and D. G. Thomas, Phys. Rev. 158, 748 (1967).
[14] J. D. Cuthbert and D. G. Thomas, Phys. Rev. 154, 763 (1967).
[15] G. F. Neumark, Phys. Rev. B 10, 1574 (1974).
[16] M. D. Sturge, A. T. Vink, and F. P. J. Kuijpers, Appl. Phys. Lett. 32, 49 (1978).
[17] M. Gundersen and W. L. Faust, Phys. Rev. B 7, 3681 (1973).

[18]F. Reif, *Fundamentals of Statistical and Thermal Physics* (McGraw-Hill, New York, 1965).
[19]M. Combescot, Phys. Status Solidi B86, 349 (1978).
[20]M. Sternheim and E. Cohen, Solid State Electron. 21, 1343 (1978).
[21]J. C. Hensel, T. G. Phillips, and G. A. Thomas, in *Solid State Physics*, edited by H. Ehrenreich *et al.* (Academic, New York, 1977), Vol. 32, p. 163.